

INDC International Nuclear Data Committee

A Study of UMC in One Dimension

Donald L. Smith

Argonne Associate of Seville
NE Division
Argonne National Laboratory
Coronado, CA, U.S.A

Denise Neudecker

XCP Division
Los Alamos National Laboratory
Los Alamos, NM, U.S.A.

Roberto Capote-Noy

Nuclear Data Section
Division of Physical and Chemical Sciences
International Atomic Energy Agency
Vienna, Austria

March 2016

Selected INDC documents may be downloaded in electronic form from
<http://www-nds.iaea.org/publications>
or sent as an e-mail attachment.

Requests for hardcopy or e-mail transmittal should be directed to
NDS.Contact-Point@iaea.org

or to:

Nuclear Data Section
International Atomic Energy Agency
Vienna International Centre
PO Box 100
1400 Vienna
Austria

Printed by the IAEA in Austria

March 2016

A Study of UMC in One Dimension

Donald L. Smith

Argonne Associate of Seville
NE Division
Argonne National Laboratory
Coronado, CA, U.S.A.

Denise Neudecker

XCP Division
Los Alamos National Laboratory
Los Alamos, NM, U.S.A.

Roberto Capote-Noy

Nuclear Data Section
Division of Physical and Chemical Sciences
International Atomic Energy Agency
Vienna, Austria

ABSTRACT

This paper discusses an investigation of the Unified Monte Carlo (UMC) approach to nuclear data evaluation that has been conducted in the framework of a single random variable (i.e., one dimension or 1-D). The hypothetical data treated in this study consist of a single theoretical (model-calculated) value and a single experimental value, along with their respective uncorrelated uncertainties. Technical complications that are inevitably encountered when considering data sets involving multiple variables, as well as complex relationships between measured experimental data and these variables, are avoided by working entirely in 1-D. Among these complications are certain effects that arise from including ratio data and integral data. Nevertheless, even in the 1-D framework it is shown that issues associated with data discrepancies, non-normal prior probability function shape effects (e.g., skewness), and stochastic convergence that arise in applying the UMC concept could be investigated readily. This has led to some interesting conclusions. Extensive graphs and tables of numerical results serve to illustrate and quantify these findings. Three variants of the UMC approach, UMC-G, UMC-G+, and UMC-B, as well as the conventional generalized least-squares (GLS) evaluation method are considered, and their predictions are compared in this 1-D framework. Some general observations that may be applicable in a broader context are provided.

Contents

1. Introduction	7
2. UMC Formalism in 1-D	9
3. A 1-D Model for Prior Probability	13
4. Statistical Studies	17
5. A Simple Evaluation Exercise	23
6. Summary	30

1. Introduction

The modern era in nuclear reaction data evaluation (henceforth referred to simply as “data evaluation”) began in the mid 1970’s with widespread implementation of the least-squares method [1]. This method enables evaluators to include theoretical (model-calculated) and experimental data in evaluations in ways deemed to be more rigorous and objective than earlier techniques. The concept of least-squares has a long history that is generally thought to have originated with Gauss [2]. However, it was also suggested by Legendre [3] who disputed Gauss’s claim of discovery. More recently, this method has been justified mathematically, within the framework of probability theory, through the work of Shannon on information theory [4] and Jaynes on the Principle of Maximum Entropy [5]. Bayes Theorem [6], first suggested by an English clergyman, Thomas Bayes, is also an essential aspect of this approach.

While there can be no doubt that use of the least-square method in data evaluation has elevated the process of data evaluation to a more objective level than previous approaches, it nevertheless suffers from some difficulties in its implementation. One difficulty that has been the object of considerable attention since the 1980’s is the so-called “Peelle’s Pertinent Puzzle” (PPP) phenomenon [7]. Various ad hoc “fixes” designed to minimize the negative impact of PPP on data evaluations that utilize the least-square method have been suggested [8]. Data evaluators have come to accept that problems of this sort are likely to be encountered in applying the least-squares method when evaluating data sets that manifest various combinations of large uncertainties, significant discrepancies, and non-linear relationships between the variables to be evaluated. Most of these difficulties can be traced to the fact that the least-squares method is based on linearization of more rigorous probabilistic formulations of the data evaluation process.

It was suggested by Smith in 1991 [1] that some of the problems associated with using the least-squares method might be avoided by utilizing an approach to data evaluation that deals directly with the underlying probability functions which govern the random variables to be evaluated. In practice this approach would involve invoking the prescriptions of Shannon and Jaynes (mentioned above) to construct the prior probability and likelihood functions needed to apply Bayes Theorem in data evaluations, and subsequently performing difficult multi-variable numerical integrations that involve these functions. Smith concluded that it was probably impractical to pursue such an approach at that time (1991) due to the inherent computational challenges. Furthermore, it was not clear then how the prior probability functions required for undertaking a Bayesian approach to data evaluation could be constructed in realistic situations. In 2004 [9] Smith suggested that stochastic (Monte Carlo) techniques might provide the means for generating information needed to construct prior probability functions, e.g., by propagating uncertainties from nuclear model parameters to calculated physical observables and even to complex systems. The rapid development of computer power and numerical data storage capacity between 1991 and 2004 had motivated Smith to reconsider the probabilistic approach to data evaluation he had mentioned thirteen years earlier. While this Monte Carlo approach provided a clear pathway for generating evaluations based solely on theory, without the consideration of experimental data [10], it was not evident in 2004 how both model-calculated data and experimental data could be included simultaneously in an evaluation scheme based entirely on Monte Carlo simulation.

A suggestion as to how this might be accomplished was offered in 2007 by Smith [11]. It was given the name Unified Monte Carlo, or UMC as an abbreviation. This approach involves

implementing Bayes Theorem within a stochastic framework. Bayes Theorem specifies that the posterior probability function p required to perform a probabilistic evaluation be constructed as the product of a prior probability function p_0 and a likelihood function L . The prior probability function p_0 should represent knowledge based solely on theory (model calculations) while the likelihood function L provides the means for introducing experimental data that are assumed to be independent of the theoretical data into the evaluation process.

Since most published experimental data sets provide estimated mean values and (hopefully) covariance data for the measurement variables, and rarely much more, an application of the prescriptions of Shannon and Jaynes [4] – [5] would suggest that the likelihood function L in applying Bayes Theorem should be a multi-variate normal distribution with respect to those variables that correspond explicitly to the measured data. In reality, this may be an overly simplistic assumption in those situations where there is good reason to expect that the provided data are not normally distributed, or if large data uncertainties that are clearly non-normally distributed are involved. Furthermore, L will definitely not be normal as a function of the variables to be evaluated if the measured data are related in a non-linear manner to the physical quantities to be evaluated, e.g., as in situations where ratio data are considered. This will be the case even when it is reasonable to assume that L can be written explicitly as a normal distribution that involves the measured variables.

As originally formulated [11], UMC requires that explicit analytical functions be specified for both p_0 and L in order to construct a posterior probability function p that can be sampled by one or other of the schemes that have been devised for use in Monte Carlo analyses. In the original formulation of UMC it was also assumed that the prior probability function p_0 should be a multi-variate normal distribution with respect to the variables to be evaluated. The mean values and covariances would be estimated by the Monte Carlo technique described in [9]. If one chooses to consider only the two lowest-order moments of the probability function, and overlook potentially important effects of higher-order moments, according to the Maximum Entropy Principle prescription, the normal distribution would indeed be the appropriate choice [5]. However, from the investigations that are summarized in [12] – [15] it became apparent that forcing the prior probability function to be normal in this manner discards potentially valuable shape information embodied in the higher-order moments of the actual probability function when it is generated by a transformation from theoretical-model variables to observable variables. For example, it neglects possible distribution asymmetry (skewness) which can have a noticeable effect on the outcome of an evaluation. Therefore, ways to circumvent this limitation of the original version of UMC needed to be found.

There is no inherent reason, when applying Bayes Theorem, for either the prior or likelihood functions to necessarily be normal. The quest to avoid the limitations of the original formulation of UMC evolved in three different directions. One approach is the original version of UMC which came to be known as UMC-G. The second approach is a modest extension of UMC-G that seeks to provide analytical functions for p_0 other than normal which predict skewness and kurtosis closer to those embodied in the “true” distribution generated by the Monte Carlo method described in [9]. For present purposes this approach is denoted as UMC-G+. The third approach stems from a novel suggestion by Capote et al. [15]. This approach came to be known as UMC-B. The historical context of the specific names “UMC-G” and “UMC-B” is also discussed in [15]. In UMC-B, a Markov Chain of observables values is generated by Monte Carlo sampling of the variables to be evaluated based on the prior probability function. This approach retains all features of the underlying probability function, associated with the derived observable variables to be evaluated, that is

generated by the transformation, performed by the model, from model parameters to the observable variables. For each of these sample values (actually vectors in realistic cases) a corresponding likelihood value is calculated based on experimental data. These likelihood values can be used to compute weighted averages that correspond to mean values, covariance matrix elements and, in principle, higher-order moments of the posterior function as well. These likelihood values can correspond to data that are normally distributed or even governed by other assumed probability distributions, e.g., the lognormal distribution. While the UMC-B approach yields prior information regarding p_0 that is devoid of approximations, it does not suggest how this information can be represented in analytical form, as required for the application of UMC-G+.

Further investigation of these three methods is clearly worth pursuing so that the strengths and limitations of the various UMC approaches can be better understood. The goal of the present work is to explore some of these issues in one dimension (i.e., in the case of a single random variable). This approach strips away many of the complexities associated with the various UMC methods, and data evaluation in general, and it enables such important matters as stochastic convergence and the effects of non-normal shapes for the prior probability function to be investigated in the purest possible context. The work reported here involved numerical studies in this simplified framework aimed at gaining a better understanding of the evaluation process, not only of issues related to stochastic convergence but also of similarities and differences in the predictions of GLS, UMC-G, UMC-G+, and UMC-B for a number of specific examples that exhibit both “typical” and “extreme” conditions. The results of the present investigation are provided here in the form of both numerical and graphical information. For convenience this tabular and graphical material is always presented as “Figures”, rather than being labelled as either “Tables” or “Figures”, since both graphical and tabular results may well appear together rather than separately.

2. UMC Formalism in 1-D

This section describes formalisms in one dimension for the various UMC approaches mentioned in Section 1 as well as one for generalized least squares (GLS). It is assumed throughout that both the theoretically calculated and measured values included in the analysis processes are directly equivalent to the variable being evaluated. It is further assumed that the theoretical model M has a single variable x that is governed by a normal probability function r_0 in the variable space $S\{x\}$. Function r_0 has a mean value x_0 and standard deviation s_x . The model M maps x to a single variable y in a distinct variable space $S\{y\}$ that corresponds to a derived observable quantity. The probability function p_0 results from the mapping by M of x to y . It has a mean value y_0 and standard deviation s_0 . These two values are treated as the model-calculated result and its uncertainty, respectively, for evaluation purposes. As mentioned in Section 1, p_0 need not be normal. In fact, it usually will not be normal. Also, most realistic mappings by M from variable x to variable y lead to prior probability functions p_0 that cannot be expressed analytically. The mapping topology described here is illustrated schematically in Fig. 1. Finally, be aware that in the present discussion r_0 , p_0 , L , and p are all continuous probability density functions.

It is also assumed in this discussion that a single hypothetical “experimental” value y_e with uncertainty (standard deviation) s_e is available for inclusion in the evaluation process along with the calculated value y_0 and its standard deviation s_0 . The experimental quantities are usually treated as parameters of a single-variable normal probability function L that governs the measurement process. The function L has the following normalized form:

$$L(y) = \exp[-0.5(y - y_e)^2 / s_e^2] / (2\pi s_e^2)^{1/2} . \quad (1)$$

Given the data value pairs (y_0, s_0) and (y_e, s_e) resulting from efforts to calculate (theoretically) and measure information about the observable quantity y , one can apply the generalized least-squares (GLS) method directly to produce an evaluated solution y_{sol} and its uncertainty (standard deviation) s_{sol} as follows [1]:

$$y_{sol} = [(y_0 / s_0^2) + (y_e / s_e^2)] / [(1 / s_0^2) + (1 / s_e^2)] , \quad (2)$$

$$(1 / s_{sol}^2) = (1 / s_0^2) + (1 / s_e^2) . \quad (3)$$

It is evident from Eqs. (2) and (3) that the evaluated result in this simple example is just the well-known mean value and standard deviation derived from weighted averaging of two independent data values, with the weighting factors defined by their respective standard deviations. Knowledge of the underlying probability distribution appears not to be required explicitly. However, this is somewhat deceptive since the validity of the GLS formalism relies on the assumption that the data being evaluated are indeed normally distributed [1].

In the UMC concept [11], the prior probability p_0 and likelihood L functions are employed to construct the posterior probability function p according to Bayes Theorem [6]:

$$p(y) = p_0(y) L(y) . \quad (4)$$

It is convenient to assume that both p_0 and L are normalized. However, the product of these two normalized functions, the posterior probability function p , is not normalized. Therefore, a normalization constant has to be determined in any applications that requires p to be normalized. However, the necessity to normalize p can often be avoided in practice [11] – [15]. The posterior probability function p embodies both the model-calculated and experimental information provide for evaluation purposes. The nature of function p can be characterized in part by its moments [1]. In particular, if a very large collection K of random values $\{y_k\}$ is generated by sampling the variable space $S\{y\}$ according to probability function p , then the four lowest-order moments of p can be derived stochastically using the following formulas:

$$m_1 \approx [\sum_{k=1, K} y_k] / K , \quad (5)$$

$$m_2 \approx [\sum_{k=1, K} (y_k - m_1)^2] / K , \quad (6)$$

$$m_3 \approx [\sum_{k=1, K} (y_k - m_1)^3] / K , \quad (7)$$

$$m_4 \approx [\sum_{k=1, K} (y_k - m_1)^4] / K . \quad (8)$$

Approximate equality “ \approx ” approaches true equality “ $=$ ” for very large samples (i.e., very large K). This effect, known as stochastic convergence, has been studied extensively in the present work, and it is discussed in the Section 4 of this paper. The reader should be reminded that some definitions given in the literature for these probability function moments involve integers other than K , e.g., $K-1$, $K-2$, $K-3$... [1]. These alternative definitions are appropriate in instances involving relatively small samples (i.e., small K), but the numerical

differences between the results obtained using these alternative formulas become negligible once K is large (e.g., usually $K > 1000$) as is generally the case in the present investigation.

UMC Topology in One Dimension

The schematic diagram shows mapping from space $S\{x\}$ to space $S\{y\}$ by the theoretical model M . The shaded areas denote regions of non-negligible probability for r_0 (green) and p_0 (blue).

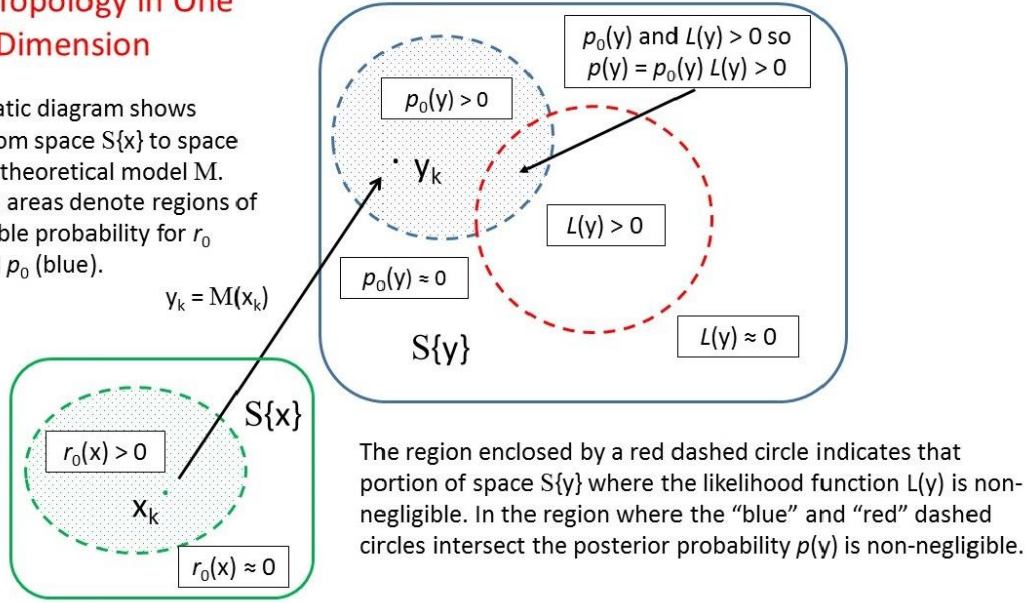


Fig. 1: Schematic diagram that shows the topology associated with mapping theoretical model parameter x to derived observable variable y for the UMC data evaluation concept.

Moment m_1 is called a “raw moment” while m_2 , m_3 , and m_4 are called “central moments” because their values depend on m_1 , i.e., they are “centered” on m_1 . These four formulas are very important for present purposes because they provide a means for evaluating these moments based only on the generated collection of random sample values $\{y_k\}$, without having to know and resort to an explicit analytic expression for p . Of course, the same approach can be applied to determine the moments of r_0 and p_0 provided that corresponding collections of random values of x or y , respectively, are available that are characteristic of these two particular probability functions. The first moment m_1 is called the mean value (MV) of p and the second moment m_2 is the variance (Var) of p .

It is common to consider standard deviation (Std), skewness (Skew), and kurtosis (Kurt) as characteristic factors in discussing the second-, third-, and fourth-order properties of probability functions such as p . They are defined as follows:

$$\text{Std} = (\text{Var})^{1/2} = m_2^{1/2}, \quad (9)$$

$$\text{Skew} = m_3/m_2^{3/2}, \quad (10)$$

$$\text{Kurt} = m_4/m_2^2. \quad (11)$$

It is noteworthy that both Skew and Kurt are dimensionless factors whereas m_1 , m_2 , Std, m_3 , and m_4 all have dimensions. Finally, it is important to point out that these formulas correspond to population moments, i.e., they are characteristic of the entire population of possible random values associated with probability function p , not just limited samples [1].

However, as mentioned above, as long as the sample size K is very large, the distinction between “population” and “sample” moments is negligible. So, unless mentioned otherwise, all moments discussed in this paper are “population” moments. Extensive use has been made of Eqs. (5) – (11) in numerical analyses performed in the present investigation, either directly or through computational algorithms included in the commercial software packages Microsoft EXCEL and MathWorks MATLAB.

If probability function p of variable y can be expressed analytically and, most important, if it is appropriately scaled to be normalized, then the following formulas can be used to evaluate MV and Std numerically:

$$MV = m_1 = \int y p(y) dy , \quad (12)$$

$$Std = [\int y^2 p(y) dy - m_1^2]^{1/2}. \quad (13)$$

The indicated integrations extend over the entire range of space $S\{y\}$ where the values of $p(y)$ are non-negligible. It is clearly evident from Eq. (4) that direct applications of Eqs. (12) and (13) require p to be normalized and expressible analytically. In the simple case of a single variable the integrals indicated in Eqs. (12) and (13) usually can be calculated numerically without too much difficulty. One approach is deterministic (D), i.e., establish a fine grid of K equally spaced values $\{y_{kD}\}$ centered in corresponding contiguous, equal-width intervals $\Delta y_k = (y_{\max} - y_{\min})/K$ that span the range (y_{\min}, y_{\max}) where the integrands are non-vanishing. Another approach is stochastic (R), i.e., Monte-Carlo integration. This involves generating a large collection of K values $\{y_{kR}\}$ selected randomly from a uniform distribution over the same range of variable y . Depending on how y_k is determined (y_{kD} or y_{kR}), if $Q(y)$ is the integrand corresponding to a particular y , the integral can be approximated for large K by:

$$\int Q(y) dy \approx \sum_{k=1, K} Q(y_{kD}) \Delta y_k \quad (\text{deterministic}) \quad (14a)$$

$$\int Q(y) dy \approx (\sum_{k=1, K} Q(y_{kR})/K) (y_{\max} - y_{\min}) \quad (\text{stochastic}) \quad (14b)$$

Eqs. (14a) and (14b) are basically the same. The deterministic approach, represented by Eq. (14a), is a reasonable choice if the function involved in the integration is “well-behaved” and does not have too long a “tail” toward either much larger or much smaller values than the region of maximum values. The stochastic approach, represented by Eq. (14b), is referred to in [11] – [15] as the “Brute Force” method of Monte Carlo integration. It is more flexible than the deterministic approach and it can be quite effective. However, it is relatively inefficient and may require a very large number K of samples. The Metropolis-Hastings sampling scheme [16] tends to be far more efficient in the sense that it concentrates sampling to values of y_k that yield the largest magnitudes for $Q(y_k)$ in the range (y_{\min}, y_{\max}) . The collection $\{y_k\}$ of these favored values of y then can be used to calculate $MV\{y\}$ and $Std\{y\}$ as well as $Skew\{y\}$ and $Kurt\{y\}$ if that is desired. Note that the notation $MV\{y\}$, $Std\{y\}$, $Skew\{y\}$, and $Kurt\{y\}$ is used throughout this paper to represent stochastic determinations of these quantities. The approach is similar for UMC-G and UMC-G+. The only difference between these two variants of UMC is that in UMC-G the prior probability function p_0 is forced to be normal, as seen in Eq. (15).

$$p_0(y) = \exp[-0.5(y - y_0)^2 / s_0^2] / (2\pi s_0^2)^{1/2}. \quad (15)$$

The parameters y_0 and s_0 that characterize p_0 are derived from the following formulas that utilize values of y from the collection $\{y_k\}$ generated by the transformation $y_k = M(x_k)$, as is discussed above and illustrated in Fig. 1:

$$y_0 = MV\{y\} = (\sum_{k=1,K} y_k)/K , \quad (16)$$

$$s_0 = Std\{y\} = \{[(\sum_{k=1,K} y_k^2)/K] - y_0^2\}^{1/2} . \quad (17)$$

It is clear that UMC-G, originally denoted as UMC in [11], ignores any higher-order moments that might be embodied in the prior probability function p_0 whenever the transformation function M involves a non-linear relationship between x and y . Although mentioned in Section 1, it is worthwhile to re-emphasize the distinctions between UMC-G and UMC-G+ to insure that confusion is avoided in the ensuing discussions. Although more recent studies of UMC-G have broadened the application of the original concept to include cases where either one or the other, or both, of the functions p_0 and L might be non-normal [12] – [15], the term “UMC-G” continues to be viewed by many people in the nuclear data community solely in the context of normal distributions. To avoid confusion, in the present work the term “UMC-G+” signifies an application of UMC-G where L is normal but p_0 is not necessarily normal but nevertheless can be represented in an analytical form. As mentioned in Section 1, Capote et al. [15] have suggested an approach to UMC referred to as UMC-B that does not require the prior probability p_0 to be either normal or to be specified in the form of an analytical function. If $\{y_k\}$ corresponds to a collection of K theoretical values y generated stochastically by the transformation $y_k = M(x_k)$, and $\{w_k\}$ represents a corresponding collection of K weighting factors based on experimental data and derived from the formula $w_k = L(y_k)$, where L is given by Eq. (1), then the joint collection of value pairs $\{y_k, w_k\}$ can be used for evaluation purposes to generate solution mean value y_{sol} and its standard deviation s_{sol} :

$$y_{sol} = (\sum_{k=1,K} w_k y_k)/(\sum_{k=1,K} w_k), \quad (18)$$

$$s_{sol} = \{[(\sum_{k=1,K} w_k y_k^2)/(\sum_{k=1,K} w_k)] - y_{sol}^2\}^{1/2} \quad (19)$$

The collection of K value pairs $\{y_k, w_k\}$ could also be used for additional calculations, e.g., for the analysis of physical systems whose performance is governed in part by these evaluated results. This would correspond to an extension of the TMC approach of Koning and Rochman [10] that takes into account both theoretical and experimental data information. It is evident from Fig. 1 that the region of space $S\{y\}$ where significant weighting values w_k would be encountered might be rather small if the model-calculated results are inconsistent with the experimental ones. That, in turn, would impact negatively on the stochastic convergence of an evaluated solution derived by the UMC-B approach. This issue is examined further in the present work through examples discussed in Section 5.

3. A 1-D Model for Prior Probability

It is of interest to explore in one dimension the influence of non-normal prior probability functions on evaluations that are likely to be involved in applying UMC-G, UMC-G+, and UMC-B. Therefore, conjuring a “toy” model M that involves a non-linear relationship between a single model parameter and a single derived variable is essential for such an investigation. To be useful for the investigation, this non-normal prior probability function should be expressible in analytical form and be amenable to some adjustment, by changing its

parameters, to produce various skewness and kurtosis values that differ significantly from the more constrained normal probability function (Skew = 0; Kurt = 3). Also, this prior probability function must be related intimately to the selected non-linear mathematical model M that transforms model variable x to derived variable y , i.e., $y = M(x)$. Throughout the present investigation x is assumed to be normally distributed, as mentioned in Section 2. Therefore, it is suggested that a useful theoretical model M for the present investigations be defined by the exponential transformation $y = \exp(c x)$, where c is a scaling constant that is assumed to have no uncertainty whereas x is uncertain. If variable z is defined as $z = c x$, it will also be normally distributed. Thus, $y = \exp(z)$. It is well established that if z is normally distributed then $y = \exp(z)$ by necessity is lognormally distributed [1]. Can the lognormal function ever be considered relevant in realistic physical situations? To address this question in the context of nuclear data evaluation, it is informative to mention three examples in nuclear science where data are seen to exhibit exponential behavior, if only over limited ranges [17-18].

The simplest example is exponential decay of radioactivity. This model is validated physically, and it takes the well-known form $A = A_0 \exp(-\lambda t)$ where $c = t$, $x = -\lambda$, and A_0 is a factor that defines intensity but does not affect the time dependence of radioactive decay. This case is discussed extensively in [18] so it is pursued no further in this paper.

The second example is illustrated in Fig. 2. It shows evaluated cross-section data from ENDF/B-VII.1 for the $^{197}\text{Au}(n,\gamma)^{198}\text{Au}$ reaction from 20 – 40 keV (blue curve), along with a small sampling of relevant experimental data. These experimental data points scatter considerably with respect to the evaluated curve, but the general trend of both the evaluation and experimental data on a linear-log scale is linear with a negative slope over this limited energy range. The red curve in this plot is a straight line on a linear-log scale which is sketched as an eye guide to the plotted data. Expressed in terms of a neutron cross section, the model would be $\sigma = \sigma_0 \exp(-\gamma E)$. Here, $c = E$ (neutron energy), $x = -\gamma$ is a model parameter that governs the slope, and σ_0 is a normalization factor.

The third example is discussed in Figs. 3 and 4. An experimental data set for the $^{58}\text{Ni}(n,p)^{58}\text{Co}$ reaction from 0.7 – 4 MeV [17] is compared in Fig. 3 with three distinct segments of exponential shapes (linear on a linear-log scale). This figure shows clearly the abrupt discontinuities in the slope of the cross section shape with energy that occur at around 1.4 and 2.7 MeV, respectively. It happens that the first-excited state (2+) of the target nucleus ^{58}Ni is situated at around 1.4 MeV while the second-excited state (4+) is situated at around 2.5 MeV. The slopes of the three distinct line segments provided as eye guides to the data, as shown in Fig. 3, are all positive for this (n,p) threshold reaction, unlike the negative slope for the ^{197}Au capture cross section, as shown in Fig. 2. These changes in cross-section shape for the (n,p) reaction are likely the result of abrupt variations in competition between the (n,p) reaction and neutron inelastic scattering due to onset of inelastic scattering contributions from individual discrete excited levels at incident neutron energies above their (n,n') thresholds.

The very sharp rise in the (n,p) cross section observed just above threshold can be attributed largely to barrier penetration considerations rather than variations in reaction channel competition. This effect can be understood by considering a simple application of the Schrodinger equation from quantum mechanics in one dimension, as described in Fig. 4. An incident particle with energy below the barrier height can penetrate the barrier even though classically this is forbidden. Uncertainty in the barrier height relative to the incident neutron energy translates in a non-linear manner to uncertainty in the calculated cross section.

The three examples discussed here suggest anecdotally that there may be situations where the lognormal function, or possibly a closely related analytical probability distribution, might on occasion be worth considering in realistic evaluation exercises even though there is no rigorous mathematical basis to support this view. An investigation of the extent to which the lognormal function and/or other analytical functions [1] might or might not be useful in characterizing the distributions derived by Monte Carlo in realistic applications would appear to merit further consideration. This exceeds the scope of the present work. However, already there is some evidence, from Figs. 2 and 3, as well as from other work in progress by one of the present co-authors (Denise Neudecker), that simplified analytical representations, e.g., by the lognormal function, of the shape of prior probability distributions generated by Monte Carlo may be worth considering in limited instances over modest energy ranges. It is suggested here that it could be useful to an evaluator, as part of the evaluation process, to examine the skewness and kurtosis of a stochastically generated prior probability distribution for model-calculated data for similarities with the skewness and kurtosis of a chosen analytical function, e.g., a lognormal function, having the same mean value and standard deviation.

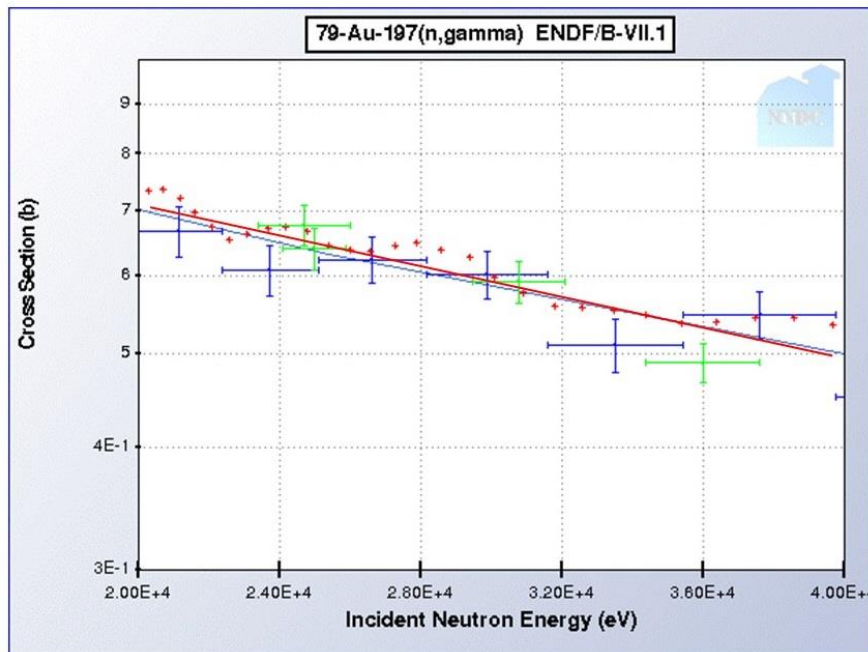


Fig. 2: Cross-sections obtained from the National Nuclear Data Center (NNDC), Brookhaven National Laboratory (<http://www.nndc.bnl.gov/sigma/>) for the $^{197}\text{Au}(n,\gamma)^{198}\text{Au}$ reaction from 20 – 40 keV. To avoid clutter, only three of the many experimental data sets available for this reaction are shown here. The blue curve is the ENDF/B-VII.1 evaluation. The red curve is a straight line (in linear-log space) drawn as an eye guide to the exhibited data.

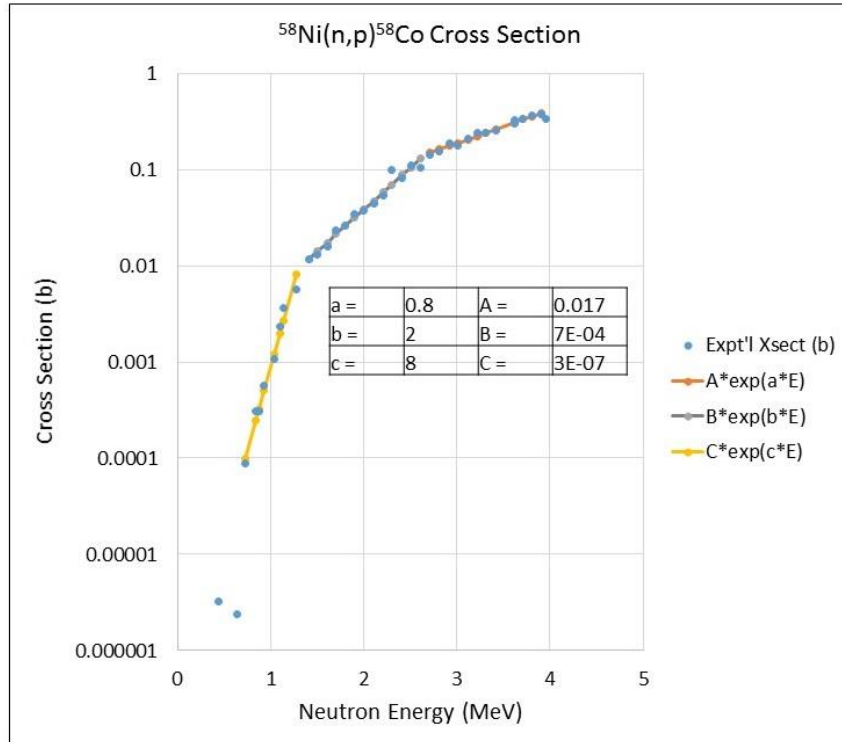
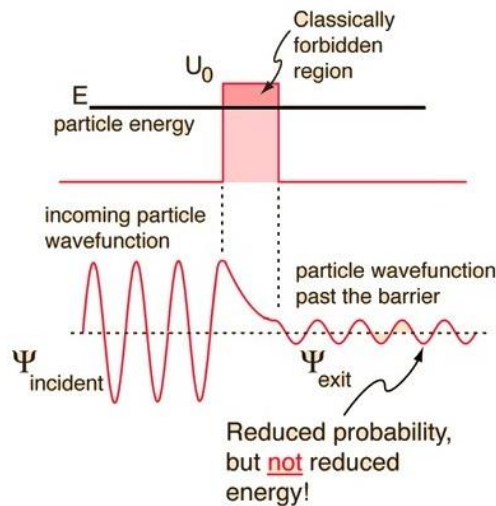


Fig. 3: Experimental cross-section data [17] for the $^{58}\text{Ni}(n,p)^{58}\text{Co}$ reaction compared with exponential cross section shapes. The “model” parameter governs the slopes in this plot.



$$\frac{-\hbar^2}{2m} \frac{\partial^2 \Psi(x)}{\partial x^2} = (E - U_0) \Psi(x)$$

$$\Psi = Ae^{-\alpha x} \text{ where } \alpha = \sqrt{\frac{2m(U_0 - E)}{\hbar^2}}$$

Fig 4: Schematic diagram that illustrates quantum mechanical barrier penetration in one dimension. The material used to prepare this figure was acquired on-line. It is associated with the HyperPhysics exploration environment, Department of Physics and Astronomy, Georgia State University (<http://hyperphysics.phy-astr.gsu.edu/hbase/quantum/barr.html>).

4. Statistical Studies

Most of the calculations performed in the present investigation and reported in this paper are stochastic (MC) in nature. Furthermore, the effects sought when comparing differences in the predictions of UMC-G, UMC-G+, UMC-B, and GLS are expected to be relatively modest. So, it is essential that the calculated results reflect adequate stochastic stability (i.e., convergence). Consequently, the fidelity of the algorithms in EXCEL and MATLAB that are used in this work to generate random samples of variables needed to be verified. The results of these numerical investigations appear in the present section.

Normal Probability Function

As discussed in Section 3, the theoretical model M that is employed in this work is $y = \exp(cx)$, with x representing the variable model parameter and c being a constant. Then, y is the derived variable that represents an observable quantity. Variable x is assumed to be normally distributed. In practice the largest standard deviation that should be considered for a normal distribution that is employed to represent an inherently positive parameter, without encountering a significant number of negative sample values, is about 30% [18]. Then the likelihood of sampling a negative number will be $< 0.1\%$. This should be acceptable for most applications since any encountered negative values can be rejected whenever they might impact an analysis in an unacceptable manner, e.g., by generating non-physical parameter values.

For purposes of the present investigation, MATLAB was used to generate 8 independent sets of samples of a variable x with sizes $K = 100, 500, 1000, 5000, 10000, 50000, 100000,$ and 500000 , respectively, for a normal distribution with mean value $x_0 = 1$ and standard deviation $s_x = 0.3$. The values $MV\{x\}$ and $Std\{x\}$ extracted from a statistical analysis of the generated random values of x were then compared with the input parameters of the normal distribution that generated these samples, i.e., x_0 and s_x . Adequate convergence is considered to exist if the moments extracted from the sample data agree with the input normal distribution parameters to within acceptable tolerances. The results from statistical analyses of these 8 independent sample data sets are provided in Fig. 5 (upper left table). It is evident that adequate stochastic convergence for present purposes is indeed achieved. From Fig. 5 (lower left table) it is also evident that the derived $MV\{x\}$ from 10 independent samples of size $K = 100000$ or greater should vary by $< 0.1\%$ while corresponding derived values of $Std\{x\}$ should vary by $< 0.2\%$. It is anticipated (although it was not tested) that adequate stochastic convergence could likely be achieved with fewer than $K = 100000$ sampling histories in cases where the standard deviation is smaller than 30%. Then the sample values would tend to cluster more closely around the mean value. Thus it can be concluded that:

It is possible to achieve quite a high degree of stochastic convergence in sampling fairly broad normal distributions (no more than 30% standard deviation) with $K = 100000$ histories. However, since computational time can be very demanding in realistic UMC evaluation, tests should be performed by the evaluator to determine the minimum number of sampling histories needed to achieve the desired accuracy.

To be on the safe side it was decided to employ $K = 500000$ histories for most of the stochastic calculations conducted in the present investigation. Whether or not such a large number of histories is necessary (or even feasible) in more realistic evaluation scenarios involving multiple variables needs to be investigated in specific situations.

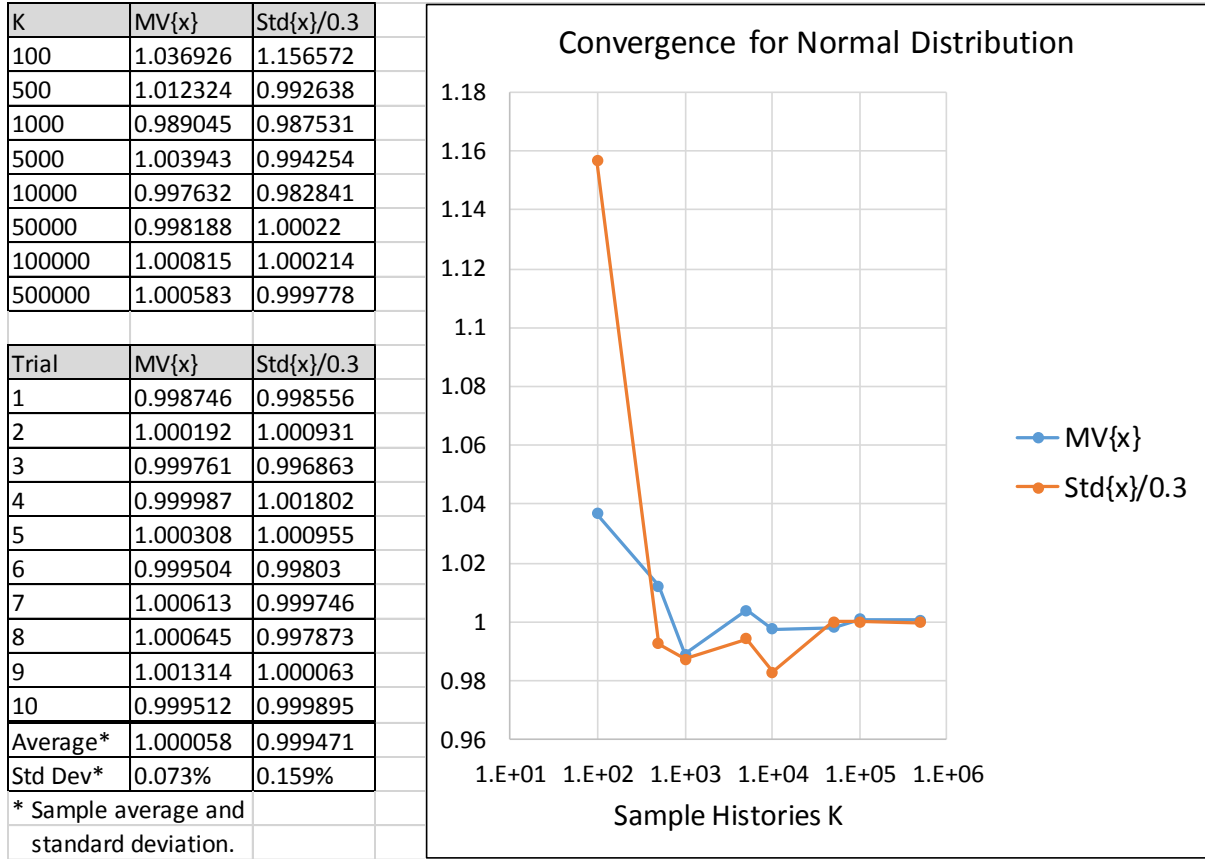


Fig 5: Stochastic convergence tests for a normal probability distribution with given mean value $x_0 = 1$ and standard deviation $s_x = 0.3$. The table at the upper-left-corner gives the values of stochastically determined $MV\{x\}$ and $Std\{x\}/0.3$ for various numbers of histories K . The same information is also displayed in the adjacent plot. The table at the lower-left-corner gives values of stochastically determined $MV\{x\}$ and $Std\{x\}/0.3$ for 10 independent trials with $K = 100000$ each. The averages and sample standard deviations of extracted $MV\{x\}$ and $Std\{x\}$ values for these 10 independent trials are also provided.

Lognormal Probability Function

Extensive use is made of the lognormal probability function in the present investigation for reasons that are discussed in Section 3. Therefore, it was considered essential for present purposes to examine the issue of statistical convergence of the stochastically derived moments for sampled collections of random variables generated by this function. As mentioned earlier, the present calculations were performed using EXCEL and MATLAB.

There is risk of confusion when naming variables in exercises such as the ones discussed here. Therefore, for present purposes m denotes the mean value of a lognormal function and v denotes the variance. Unlike the case of normal distributions, m and v are not the inherent parameters of the lognormal distribution. Consequently, μ and σ are used to denote these inherent parameters. Here, y is the random variable of the lognormal distribution and $\ln y$ is the natural logarithm of y . The normalized lognormal prior probability function is:

$$p_0(y) = \exp[-0.5 (\ln y - \mu)^2 / \sigma^2] / (2\pi\sigma^2 y^2)^{1/2} . \quad (20)$$

If the mean value m and variance v are given for the lognormal function p_0 of Eq. (20), the following formulas serve to define the relationships between m , v , μ , and σ [19] – [20]:

$$\mu = \ln[m^2/(v + m^2)^{1/2}], \quad (21)$$

$$\sigma = \{\ln[(v/m^2) + 1]\}^{1/2}, \quad (22)$$

$$m = \exp[\mu + (\sigma^2/2)], \quad (23)$$

$$v = \exp(2\mu + \sigma^2) [\exp(\sigma^2) - 1]. \quad (24)$$

Analytical expressions for the higher moments of lognormal p_0 of interest here are:

$$\text{Skew} = [\exp(\sigma^2) + 2] [\exp(\sigma^2) - 1]^{1/2}, \quad (25)$$

$$\text{Kurt} = \exp(4\sigma^2) + 2 \exp(3\sigma^2) + 3 \exp(2\sigma^2) - 3. \quad (26)$$

Since analytical expressions do exist for all the mathematical quantities of interest for present purposes in studying the lognormal function, this enables direct comparisons to be made between exact and stochastic determinations of these quantities, providing convenient tests of convergence. This is one of several features of this probability function that make it very well suited for the present investigation.

The following relationships between variables and constants are defined as in Section 3: $z = c x$; $y = \exp(z)$. As mentioned above, it is assumed that x is normally distributed with $x_0 = 1$ and $s_x = 0.3$. The stochastic and analytical computations that are discussed in this section proceeded according to the following steps: 1) A specific constant value c is selected. 2) A random collection of 500000 normally distributed values $\{x_k\}$ is generated. 3) This collection is used to produce a corresponding set of 500000 values $\{z_k\}$ based on the magnitude of the constant c . 4) The collection $\{z_k\}$ is used to calculate a collection of 500000 derived values $\{y_k\}$. 5) The mean value $MV\{y\}$ and variance $\text{Var}\{y\}$ are deduced stochastically from the random collection $\{y_k\}$. 6) Values of skewness $\text{Skew}\{y\}$ and kurtosis $\text{Kurt}\{y\}$ are also deduced from this random collection of $\{y_k\}$. 7) The values of $MV\{y\}$ (which corresponds to m , as introduced above) and $\text{Var}\{y\}$ (which corresponds to v , also introduced above) are then used to derive the parameters of an analytic expression for the lognormal probability, i.e., μ and σ , according to Eqs. (21) and (22), respectively. 8) Values of the skewness and kurtosis are then calculated analytically using Eqs. (25) and (26), respectively, for comparison with the corresponding stochastically determined values.

This 8-step process was repeated 18 times for 18 distinct values of c ranging from 0.01 to 5. The numerical results from these computations are compiled in Fig. 6. The skewness and kurtosis results are also plotted in Fig. 7.

Fig. 8 compares histograms for the lognormal probability functions corresponding to $c = 1$ and $c = 2$, respectively. The distribution for $c = 2$ has a much longer “tail” toward high y values than for $c = 1$. The shape of the histograms for smaller values of c resemble normal distributions closely while those for large values c are even more strongly skewed toward large y values than is seen for the histograms shown in Fig. 8.

c	MV{y}	Var{y}	SD{y} (%)	MC Skew{y}	Calc Skew{y}	Skew{y} Ratio	MC Kurt{y}	Calc Kurt{y}	Kurt{y} Ratio
0.01	1.01005326	9.20334E-06	0.30%	0.009546661	0.009010545	1.059498754	2.986482268	3.000144338	0.995446196
0.02	1.02022148	3.7423E-05	0.60%	0.018360323	0.017988773	1.020654543	3.005848306	3.000575287	1.001757336
0.05	1.051397105	0.000249424	1.50%	0.050431397	0.045066778	1.119037124	3.012155407	3.003610913	1.002844741
0.08	1.083637273	0.000675904	2.40%	0.071290718	0.071988494	0.990307114	3.011111659	3.009214491	1.000630453
0.1	1.105688395	0.001099938	3.00%	0.092645569	0.090012521	1.029252011	3.020753971	3.014407518	1.002105373
0.2	1.223565577	0.005387621	6.00%	0.181803031	0.180182729	1.008992549	3.057862507	3.057773321	1.000029167
0.5	1.667057935	0.063333755	15.10%	0.456415656	0.456325589	1.000197376	3.3602307	3.372492876	0.996364062
0.8	2.291590108	0.310992511	24.34%	0.741827423	0.744472885	0.99644653	3.962082894	4.001402146	0.990173631
1	2.843910078	0.760982611	30.67%	0.94751543	0.949083525	0.99834778	4.635005222	4.643308251	0.998211829
1.2	3.541520673	1.745112913	37.30%	1.176602706	1.170933723	1.004841421	5.607349068	5.533123532	1.013414762
1.5	4.963403071	5.544857513	47.44%	1.548896369	1.53005045	1.012317188	7.574849791	7.432109422	1.019205903
1.8	6.997151043	16.5276669	58.10%	1.922346205	1.939168004	0.991325249	9.9361647	10.35432642	0.959614783
2	8.820263591	33.53282769	65.65%	2.248167508	2.25256838	0.998046287	12.9965565	13.1982634	0.984717164
2.5	16.16218706	196.7568843	86.79%	3.191198276	3.257395063	0.979677999	24.05191375	26.44817983	0.909397694
2.8	23.40940673	562.4538655	101.31%	3.987951017	4.079127432	0.977648059	36.86542866	42.82081823	0.860923032
3	30.16506088	1146.453619	112.25%	4.903557147	4.781641284	1.025496656	60.83093613	61.4908388	0.989268277
4	111.7935094	39579.78974	177.96%	8.860949972	10.97463575	0.807402649	172.903277	495.2832708	0.349099772
5	460.3803435	1873958.303	297.35%	24.77944123	35.21034068	0.703754657	1442.902757	11574.91814	0.124657707

Fig. 6: Compiled analytical and stochastic results for a lognormal probability function. Examination of the MC/Calc Skew and Kurt ratios provides an indication of the quality of stochastic conversion to the true values of Skew and Kurt versus “c” for $K = 500000$ histories.

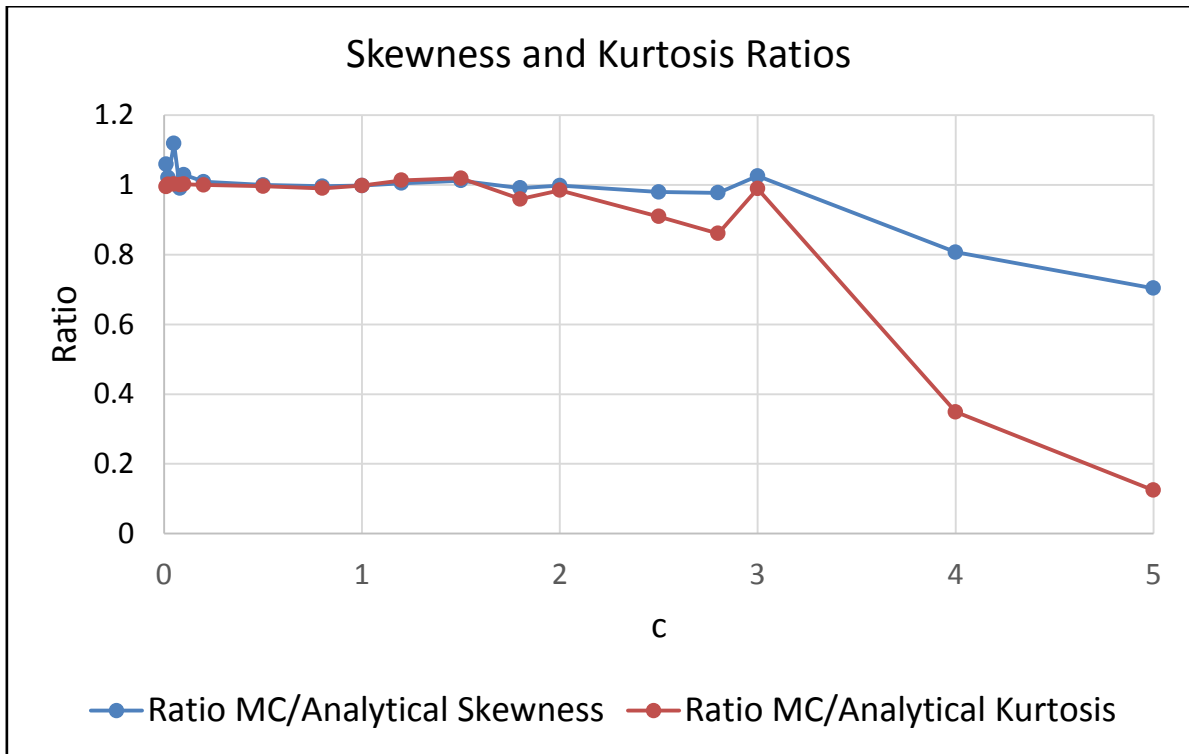


Fig. 7: Plotted ratios of stochastically determined and analytically calculated skewness and kurtosis factors for a lognormal distribution based on values taken from the table in Fig. 6.

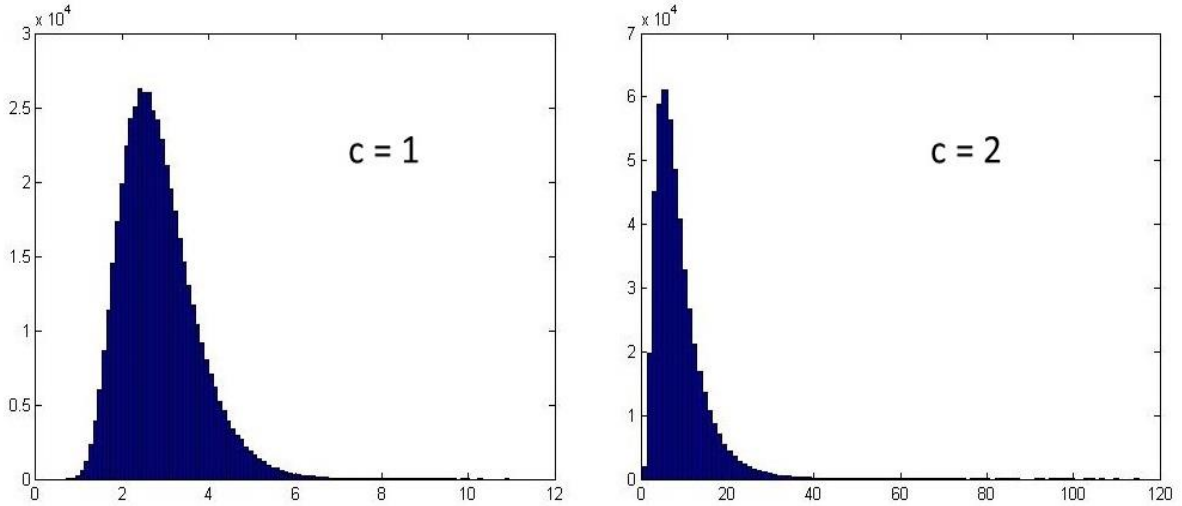


Fig. 8: Histograms of 500000 values of y , as generated with the formula $y = \exp(c x)$, for $c = 1$ and $c = 2$, respectively. The random values of y were generated by sampling normally-distributed x with mean value $x_0 = 1$ and standard deviation $s_x = 0.3$ (30%).

It is evident from Fig. 7 that a stochastic (MC) analysis of 500000 values $\{y_k\}$ that are lognormally distributed yields results for $\text{Skew}\{y\}$ and $\text{Kurt}\{y\}$ that agree very well with the analytical values for $c = 1$ or less, with the exception of $\text{Skew}\{y\}$ whenever c is close to zero. The reason for instability of skewness for very low values of c is that it is difficult to determine this factor stochastically when it is very close to zero, as is the case for small values of c . The agreement between MC and analytical results for $\text{Skew}\{y\}$ is adequate up to $c = 3$ but the MC/Calc ratios depart from unity toward significantly lower values at higher values of c . In the case of $\text{Kurt}\{y\}$, the agreement is adequate up to $c = 2$ but the MC/Calc ratios depart dramatically from unity toward lower values at values for $c > 3$. It should be apparent qualitatively from an inspection of Eqs. (5) – (8) why it is more difficult to achieve stochastic convergence when calculating skewness and kurtosis for functions such as the lognormal than it is when calculating mean values and standard deviations. This should not be a problem for most practical data evaluation scenarios since it is clear from Fig. 6 that the uncertainties (standard deviations) for the lognormal function are quite large when $c > 2$, and uncertainties of this magnitude are not very likely to be encountered in typical nuclear data evaluation scenarios except in specialized cases, e.g., those encountered in data pertinent to nuclear astrophysics. Nevertheless, evaluators should be aware that if they are required to deal with these more extreme situations, including those involving large uncertainties and discrepant data, poor overlaps between the prior and likelihood distribution functions are likely to signal that there will be difficulties in achieving adequate sampling of the product function, according to Bayes Theorem, especially when employing an evaluation approach such as UMC-B. This scenario could lead to questionable outcomes for their evaluations.

The stability of $\text{MV}\{y\}$, $\text{Std}\{y\}$, $\text{Skew}\{y\}$, and $\text{Kurt}\{y\}$ for $c = 2$ was investigated next by considering 10 independent MC trials that are all based on the same input parameters. The results are given in Fig. 9.

Trial #	MV{y}	Std{y}	Std{y} %	Skew{y}	Kurt{y}
1	8.817378	5.788671	65.651%	2.251247	13.39604
2	8.811111	5.785255	65.659%	2.230343	12.61108
3	8.825292	5.790037	65.607%	2.21997	12.63176
4	8.806791	5.759584	65.399%	2.197635	12.39435
5	8.814009	5.801598	65.822%	2.326604	14.49515
6	8.811244	5.776718	65.561%	2.208617	12.35653
7	8.820369	5.801016	65.768%	2.273965	13.3431
8	8.805842	5.758799	65.397%	2.192463	12.2124
9	8.819524	5.788721	65.635%	2.314145	14.26671
10	8.819148	5.792554	65.682%	2.290151	13.88673
Average *	8.815071	5.784295	65.618%	2.250514	13.15938
Std Dev *	0.00632	0.015048	0.138%	0.048559	0.838972
Std Dev %	0.072%	0.260%	0.210%	2.158%	6.375%
* Sample averages and standard deviations.					

Fig. 9: The results of 10 independent trials of 500000 histories each that sample a lognormal distribution with designated fixed input mean value $y_0 = 8.8203$ and standard deviation $s_0 = 5.7908$. The averages and sample standard deviations of the 10 stochastically obtained values for MV{y}, Std{y}, Skew{y}, and Kurt{y} are seen at the bottom of the table.

The preceding calculations all involve non-negative values of c . However, it has been determined that the same discussion is applicable if negative values of c with comparable magnitudes are considered. For example, the results of 500000 MC calculations employed to generate the moments of lognormal distributions with $c = 1$ and -1 , respectively, are shown in Fig. 10. It is seen that while the absolute magnitudes of the mean values and standard deviations are quite different, for obvious reasons, the percent standard deviation, the skewness, and the kurtosis are the same within statistical uncertainties regardless of the sign of c .

Independence of the shape of the generated lognormal probability distribution with respect to the sign of c is also evident from inspection of a plot of the histogram generated with $c = -1$, as shown in Fig. 11. The shape of that histogram is obviously visually the same as the one shown for $c = 1$ in Fig. 8. This outcome offers mathematical evidence that the lognormal function can serve as a reasonable prior probability function when the data behave exponentially and exhibit either positive or negative slopes when plotted on a linear-log scale.

c	MV{y}	Std{y}	Std{y} %	Skew{y}	Kurt{y}
-1	0.384608	0.11809	30.704%	0.96024	4.718317
1	2.843389	0.872303	30.678%	0.949703	4.644493

Fig 10: Comparison of moments of a lognormal probability function for $c = 1$ and $c = -1$.

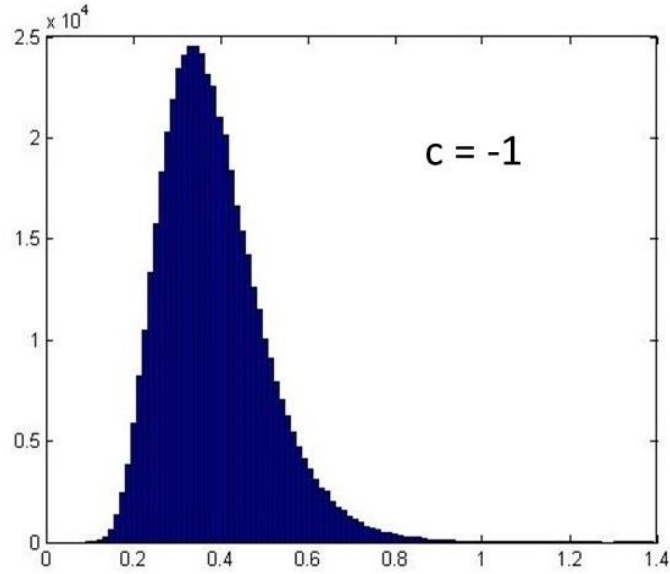


Fig. 11: Histogram of the prior probability function that corresponds to $c = -1$.

The general conclusion that can be deduced from the present exercises involving the lognormal distribution is as follows:

Data that demonstrate a linear dependence on a logarithmic scale over a range of derived variables, regardless of whether the slope is positive or negative, can be described reasonably well statistically using a lognormal distribution, although a large number of histories K might be needed to compute skewness and kurtosis factors reliably when the percent standard deviation is relatively large.

5. A Simple Evaluation Exercise

This section describes the evaluation of a variable y for which there exist a model calculated data point (y_0, s_0) and an experimental data point (y_e, s_e) to be considered. As indicated above, “ y ” denotes mean value and “ s ” denotes standard deviation for each of these data points. Furthermore, these two data points are independent. The solution results are denoted by (y_{sol}, s_{sol}) . Four evaluation techniques discussed in this paper have been employed in the present analyses: GLS, UMC-G, UMC-G+, and UMC-B. Various combinations of numerical values for the input data are treated by these methods.

The GLS solution is obtained using Eqs. (2) and (3). It is treated in the present investigation as the “benchmark” solution to which the results obtained using the three UMC methods are compared. GLS is not chosen as the benchmark with the assumption that it is always the “best” solution but rather because the GLS solution results are obtained analytically and thus are not affected to any extent by imprecision that is inevitably associated in calculating integrals numerically and/or by unpredictable stochastic effects.

While UMC-G in general is conceived as a strictly Monte Carlo technique, its application for a single variable amounts essentially to performing Monte Carlo integration with respect integrands that involve the posterior probability p and various powers of the variable y . The same is true for UMC-G+. For present purposes, this amounts to performing the integrations indicated in Eqs. (12) and (13). While these calculations indeed could be performed by Monte Carlo, in the case of a single variable with a well-defined analytical expression for p it is

reasonable to evaluate these integrals using a straightforward numerical approach that involves defining fine integration meshes, as discussed in Section 2, knowing that this approach should generate essentially the same answers as Monte Carlo evaluation of the integrals using a large number of histories K . Of course, the use of Monte Carlo integration is generally a necessity in realistic multiple-variable evaluation exercises. An assumption is made in the present work, for both UMC-G and UMC-G+. Eqs. (27) and (28) below apply only when function p is normalized.

$$MV\{y\} = m_1 = \int y p(y) dy \approx [\sum_{i=1,N} y_i p(y_i) / N] R , \quad (27)$$

$$Std\{y\} = [\int y^2 p(y) dy - m_1^2]^{1/2} \approx \{[\sum_{i=1,N} y_i^2 p(y_i) / N] R - m_1^2\}^{1/2} , \quad (28)$$

where $y_i = (i-0.5)(R/N)$ for $(i = 1,N)$. For the present investigation it was determined that $N = 1000$ provided a sufficiently fine grid for calculating the integrals numerically to the accuracy desired. The continuous interval $(0,R)$ for the variable y is chosen with a sufficient width so that the integrands of all the integrals to be evaluated are effectively negligible outside this range. For this to be the case, both the prior probability function p_0 and the likelihood L function must be effectively negligible outside this range as well as the posterior function p . For convenience, liberty is taken here of using the nomenclature $MV\{y\}$ and $Std\{y\}$, which elsewhere in the present report is used to denote results from stochastic analyses, to refer specifically to the results of deterministic calculations performed using Eqs. (27) and (28).

In UMC-G, p_0 is assumed to be normal whereas in UMC-G+ it can be an arbitrary probability function of a single variable which, nevertheless, can be expressed analytically. As discussed at length in Section 3, for illustrative purposes p_0 is taken to be a lognormal function in the present investigation. As mentioned earlier, both p_0 and L should be normalized to unity. However, their product function, p , is not automatically normalized to unity. Therefore, the integral $\int p(y)dy$ is a useful quantitative measure of the overlap of the functions p_0 and L in y space. In this report this integral is given the name ‘‘Overlap’’. The magnitude of factor ‘‘Overlap’’ is an important consideration in applying the UMC-B approach, as is illustrated in Fig. 1. It is convenient that in situations where both p_0 and L are normal probability functions, the analytic formula of Eq. (29) can be employed to give an exact value for factor ‘‘Overlap’’ that can be compared readily with the result from numerical integration [21]. However, Eq. (29) does not apply if either p_0 or L (or both functions) are non-normal.

$$Overlap = \int p(y) dy = \exp[-0.5(y_0-y_e)^2/(s_0^2+s_e^2)] / [2\pi(s_0^2+s_e^2)]^{1/2} . \quad (29)$$

The evaluated predictions from GLS and UMC-G for several choices of (y_0,s_0) and (y_e,s_e) are presented in Fig. 12.

y_0	s_0 (%)	y_e	s_e (%)	Overlap*	Eval MV GLS	Eval Std GLS %	Eval MV UMC-G	Eval Std UMC-G %
30	20.00%	40	10.00%	0.0211503	36.92307692	9.014%	36.92307692	9.014%
40	10.00%	30	20.00%	0.0211503	36.92307692	9.014%	36.92307692	9.014%
30	20.00%	50	10.00%	0.0019245	41.80327869	9.189%	41.80327869	9.189%
50	10.00%	30	20.00%	0.0019245	41.80327869	9.189%	41.80327869	9.189%
30	20.00%	35	10.00%	0.0443251	33.73056995	8.963%	33.73056995	8.963%
35	10.00%	30	20.00%	0.0443251	33.73056995	8.963%	33.73056995	8.963%
30	20.00%	30	10.00%	0.0594708	30	8.944%	30	8.944%
30	10.00%	30	20.00%	0.0594708	30	8.944%	30	8.944%
30	10.00%	30	10.00%	0.0940316	30	7.071%	30	7.071%
30	20.00%	30	20.00%	0.0470158	30	14.142%	30	14.142%
30	20.00%	50	20.00%	0.0078609	35.29411765	14.577%	35.29411765	14.577%
50	20.00%	30	20.00%	0.0078609	35.29411765	14.577%	35.29411765	14.577%
30	10.00%	50	10.00%	0.0001908	35.29411765	7.289%	35.29411765	7.289%
50	10.00%	30	10.00%	0.0001908	35.29411765	7.289%	35.29411765	7.289%
20	5.00%	20	5.00%	0.2820948	20	3.536%	20	3.536%
20	1.00%	20	1.00%	1.410474	20	0.707%	20	0.707%

Fig. 12: Summary of GLS and UMC-G solutions for a simple evaluation exercise with one model-calculated value and one experimental value. MV GLS and Std GLS represent the GLS solution values for y_{sol} and s_{sob} respectively, while MV UMC-G and Std UMC-G represent the UMC-G solution values for y_{sol} and s_{sob} respectively.

*Factor ‘‘Overlap’’ is calculated by integrating the posterior probability function p numerically.

It is evident from Fig. 12 that the solution values for UMC-G that are calculated by numerical integration agree perfectly with the GLS solutions. Thus, it can be concluded that:

When the variables to be evaluated are linearly related to both the prior model-calculated data and the experimental data, the GLS evaluation approach will yield the same results as can be obtained by resorting to probabilistic approaches, such as those referred to as ‘‘UMC’’, as long as the normal distribution applies to all the input data.

This is consistent with the observation from earlier investigations for evaluations that involve experimental data which correspond directly with the model calculated prior values of the variable(s) being evaluated [11] – [15]. It was also determined in the present investigation that the values of factor ‘‘Overlap’’ determined by numerical integration agree perfectly with those obtained from the formula in Eq. (29) when the calculations are performed with a mesh size $N = 1000$. To test the sensitivity of the calculated results for factor ‘‘Overlap’’ and the UMC-G evaluations to grid size N , these calculations were also performed using smaller grid sizes. It was determined that while the agreement for smaller N remains fairly good between the UMC-G and GLS results for coarser grids ($N < 1000$), they not quite as good as when the finer grid size ($N = 1000$) is employed. For interest, Fig. 13 shows plots of p_0 , L , and p for the case $y_0 = 30$, s_0 (%) = 20%, $y_e = 40$, s_e (%) = 10%, and $R = 80$ when p_0 and L are both normal.

It should be understood that just because the evaluated results obtained from GLS and UMC-G agree perfectly this does not guarantee that these results will be physically reasonable. If the prior calculated and experimental values differ significantly, based on consideration of their respective uncertainties (i.e., they are discrepant), then an effort should be made by the

evaluator to resolve the discrepancy. Large values of chi-square or very small values of factor “Overlap” are signals of potential data inconsistency that should be investigated further.

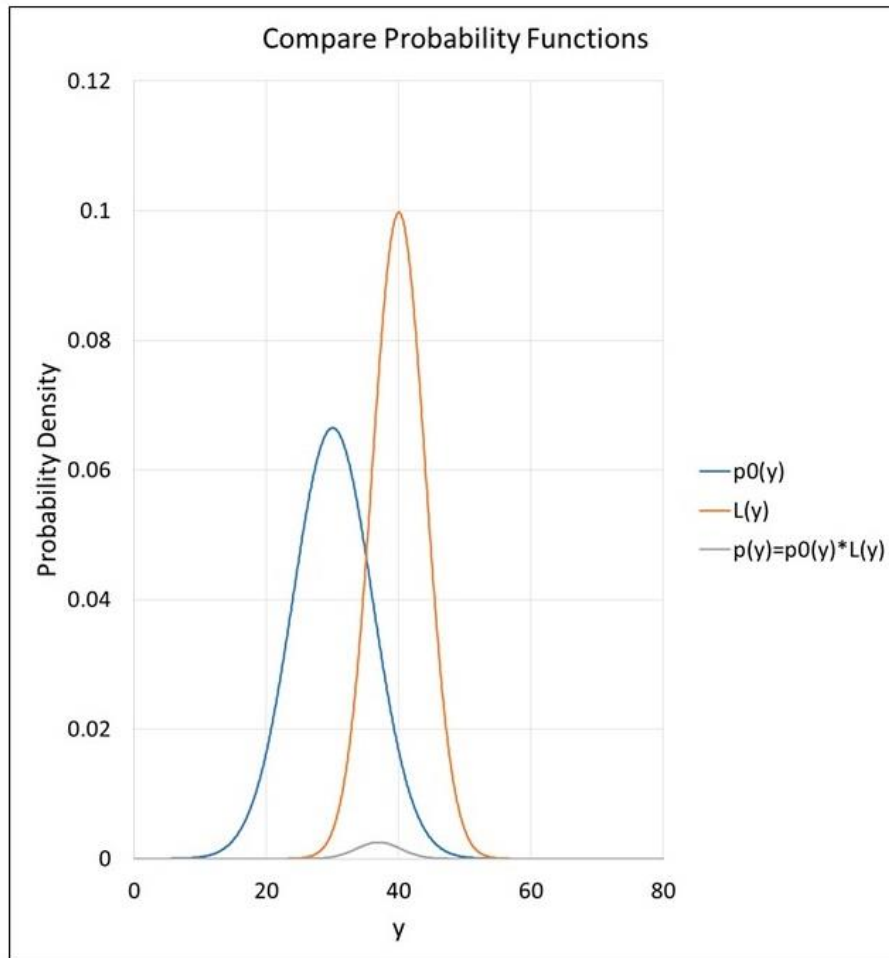


Fig. 13: Representative plots of p_0 , L , and p for $y_0 = 30$, $s_0 (\%) = 20\%$, $y_e = 40$, $s_e (\%) = 10\%$, and $R = 80$. All three probability density functions are normal in this example. The computed value of factor “Overlap” is 0.02115.

Next, a comparison is made between the GLS solutions and the UMC-G+ solutions for the same input data shown in Fig. 12. The approach to the calculations is identical to that discussed in comparing GLS and UMC-G. The only difference for UMC-G+ lies in the fact that the prior probability function p_0 need not be normal. In the present situation it is assumed to be lognormal. The results appear in Fig. 14. As mentioned above, Eq. (29) for factor “Overlap” applies only when two normal probability distributions are multiplied and not when a lognormal probability function is multiplied by a normal probability function. So the value of factor “Overlap” for p_0 and L , i.e., the integral of the posterior function p , can be obtained in the case of UMC-G+ only by numerical integration, by following the procedure described above. These values of factor “Overlap” also appear in Fig. 14. For interest, Fig. 15 shows plots of p_0 , L , and p for the case $y_0 = 50$, $s_0 (\%) = 10\%$, $y_e = 30$, $s_e (\%) = 10\%$, and $R = 80$ when p_0 is lognormal. Since p_0 and L do not overlap very well it is not possible to observe the product function p when it is attempted to show it on a linear plot.

Fig. 14 illustrates several features of the UMC-G+ results when compared with GLS for the same input data. One obvious feature is that when factor “Overlap” is very small, the differences between UMC-G+ and GLS are more noticeable. Small magnitudes of factor “Overlap” signifies that the two data values are relatively inconsistent, considering the assigned uncertainties. Another interesting feature is that the UMC-G+ results differ somewhat depending on whether $y_e > y_0$ or $y_e < y_0$. This unusual effect can be explained by the fact that the shape of p_0 is different on the low-y side than it is on the high-y side. This affects the overlap of prior p_0 with the experimental likelihood probability L . Differences in corresponding values of factor “Overlap” also reflect this phenomenon.

	y_0	s_0 (%)	y_e	s_e (%)	Overlap*	MV GLS	Std GLS %	MV UMC-G+	Std UMC-G+ %	Ratio MV	Ratio Std	
	30	20.00%	40	10.00%	0.0190129	36.92307692	9.014%	37.14065267	9.724%	1.005893	1.078811	
	40	10.00%	30	20.00%	0.0213724	36.92307692	9.014%	37.05673941	8.264%	1.00362	0.916848	
	30	20.00%	50	10.00%	0.0025887	41.80327869	9.189%	43.80972484	10.418%	1.047997	1.133802	
	50	10.00%	30	20.00%	0.0016995	41.80327869	9.189%	42.77564051	7.736%	1.02326	0.841878	
	30	20.00%	35	10.00%	0.0397722	33.73056995	8.963%	33.52838982	9.370%	0.994006	1.045438	
	35	10.00%	30	20.00%	0.044834	33.73056995	8.963%	33.69451338	8.577%	0.998931	0.957001	
	30	20.00%	30	10.00%	0.0602305	30	8.944%	29.71330675	9.006%	0.990444	1.006908	
	30	10.00%	30	20.00%	0.0595092	30	8.944%	29.92870261	8.922%	0.997623	0.997465	
	30	10.00%	30	10.00%	0.0942793	30	7.071%	29.88855837	7.067%	0.996285	0.999355	
	30	20.00%	30	20.00%	0.047499	30	14.142%	29.56654661	14.103%	0.985552	0.9972	
	30	20.00%	50	20.00%	0.0077665	35.29411765	14.577%	35.88095919	17.137%	1.016627	1.175593	
	50	20.00%	30	20.00%	0.007376	35.29411765	14.577%	36.80783716	11.875%	1.042889	0.814651	
	30	10.00%	50	10.00%	0.000237	35.29411765	7.289%	36.35885879	8.628%	1.030168	1.183794	
	50	10.00%	30	10.00%	6.366E-05	35.29411765	7.289%	37.08165446	5.941%	1.050647	0.815163	
	20	5.00%	20	5.00%	0.2822817	20	3.536%	19.98129435	3.535%	0.999065	0.999842	
	20	1.00%	20	1.00%	1.4105114	20	0.707%	19.99925007	0.707%	0.999963	0.999994	
"MV" is the evaluated solution mean value						"Std" is the evaluated solution standard deviation						
	Likelihood value is the largest - Prior value is the smallest							Note: Ratio MV and Ratio Std				
	Likelihood value is the smallest - Prior value is the largest							correspond to (UMC-G+/GLS)				
	Likelihood and experimental values both the same											

Fig. 14: Summary of GLS and UMC-G+ solutions for a simple evaluation exercise with one model-calculated value and one experimental value. MV GLS and Std GLS represent the GLS solution values y_{sol} and s_{sob} respectively, while MV UMC-G+ and Std UMC-G+ represent the UMC-G+ solution values y_{sol} and s_{sob} respectively. Ratios of MV and Std for UMC-G+ relative to GLS are also provided to show the differences in their predicted solutions.

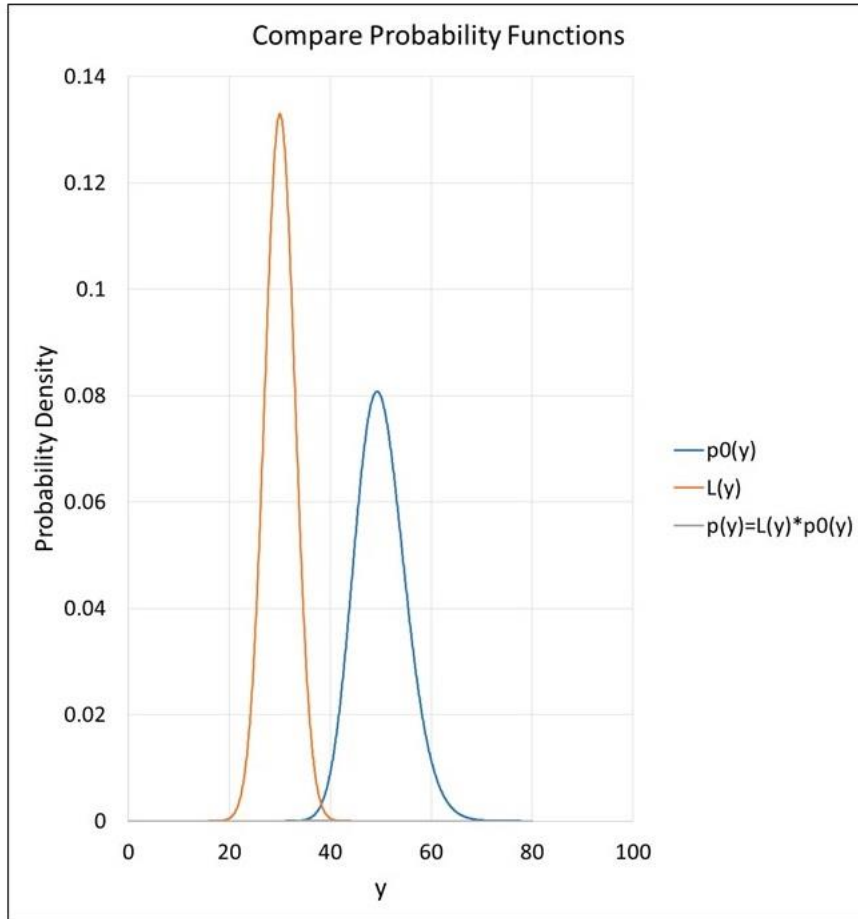


Fig. 15: Representative plots of p_0 , L , and p for $y_0 = 50$, $s_0 (\%) = 10\%$, $y_e = 30$, $s_e (\%) = 10\%$, and $R = 100$. The magnitude of factor “Overlap” is very small ($6.37E-05$) so the posterior function p is not visible in this linear plot.

It is seen from Fig. 14 is that the differences between the UMC-G+ and GLS results for the standard deviations (Std) are more pronounced than they are for the mean values (MV). While the differences appearing in Fig. 14 are generally not very large considering the given uncertainties, they do indicate that a prior probability function p_0 that exhibits skewness (and possibly kurtosis) can influence the evaluated results (both mean values and standard deviations), even in the simple case of one variable and two data values that correspond directly to the variable being evaluated. Earlier studies [11] – [15] showed that the effects of non-linearity can be quite influential when the input data, especially experimental data, do not correspond directly to the evaluated variables, e.g., in the case of ratio data, but it had not been observed previously in the case of simple data that are directly related to the evaluated variables. Thus:

One or other version of UMC should probably be employed in evaluations where the data being evaluated appear to be somewhat inconsistent based on the given uncertainties, or where it is anticipated that the prior probability function exhibits significant skewness that suggests a noticeable departure from a normal distribution.

Finally, a comparison is made in Fig. 16 between an evaluation that uses GLS, UMC-G+, and UMC-B with one variable, one model data value, and one experimental data value.

Input Data*				UMC-B			UMC-G+				GLS		
y_0	s_0 %	y_e	s_e %	MV	Std	STD %	MV	Std	Std %	Overlap	MV	Std	Std %
NHIST = 500000													
2.721694052	5.001%	2.1	19.048%	2.658334	0.124722	4.692%	2.658321	0.124792	4.694%	0.320147	2.657183	0.128851	4.849%
2.721725317	5.005%	2.1	19.048%	2.658282	0.124793	4.694%	2.658244	0.124891	4.698%	0.320149	2.657102	0.12896	4.853%
2.721906974	5.001%	2.1	19.048%	2.658522	0.124776	4.693%	2.658502	0.124802	4.694%	0.319913	2.657362	0.128863	4.849%
2.844875516	30.687%	2.1	4.762%	2.108891	0.098666	4.679%	2.108854	0.098561	4.674%	0.432174	2.109647	0.09935	4.709%
2.721629397	5.010%	2.1	4.762%	2.349627	0.072844	3.100%	2.347617	0.073903	3.148%	0.00161	2.317433	0.080636	3.480%
2.721761597	5.003%	1.9	4.737%	2.170631	0.079175	3.648%	2.205679	0.06697	3.036%	1.35E-06	2.149851	0.075082	3.492%
2.721578319	4.999%	1.9	4.737%	2.245341	0.045357	2.020%	2.20587	0.066953	3.035%	1.34E-06	2.150068	0.075064	3.491%
2.721547224	5.003%	1.9	4.737%	2.235477	0.053426	2.390%	2.205627	0.066969	3.036%	1.36E-06	2.149826	0.075079	3.492%
NHIST = 100000													
2.72206604	5.016%	2.1	19.048%	2.658241	0.12521	4.710%	2.65829	0.125135	4.707%	0.319862	2.657138	0.129229	4.863%
2.72191458	5.009%	2.1	19.048%	2.658303	0.125045	4.704%	2.658322	0.124978	4.701%	0.319971	2.657176	0.129055	4.857%
2.721592799	5.010%	2.1	19.048%	2.658023	0.125156	4.709%	2.658033	0.124977	4.702%	0.32033	2.656889	0.129054	4.857%
2.721739518	5.008%	1.9	4.737%	2.233922	0.049202	2.202%	2.205353	0.066992	3.038%	1.37E-06	2.149523	0.075103	3.494%
2.721725321	4.987%	1.9	4.737%	2.26098	0.03926	1.736%	2.206734	0.066897	3.032%	1.28E-06	2.150925	0.07501	3.487%
2.721842541	4.993%	1.9	4.737%	2.234708	0.047073	2.106%	2.206394	0.066923	3.033%	1.3E-06	2.150566	0.075036	3.489%
NHIST = 10000													
2.72139842	4.890%	2.1	19.048%	2.66074	0.121955	4.583%	2.66052	0.126282	4.748%	0.319599	2.659464	0.126282	4.748%
2.722590523	5.073%	2.1	19.048%	2.657042	0.127285	4.790%	2.657468	0.12634	4.754%	0.319739	2.656269	0.130553	4.915%
2.721070041	4.961%	2.1	19.048%	2.658603	0.123726	4.654%	2.658662	0.123939	4.662%	0.320522	2.657558	0.127914	4.813%
2.72426091	5.012%	1.9	4.737%	2.27178	0.040361	1.777%	2.205784	0.067016	3.038%	1.29E-06	2.149641	0.075145	3.496%
2.721136333	5.023%	1.9	4.737%	2.257667	0.025191	1.116%	2.204099	0.067064	3.043%	1.48E-06	2.148329	0.075169	3.499%
2.720583524	5.003%	1.9	4.737%	2.278928	0.034144	1.498%	2.205323	0.066969	3.037%	1.4E-06	2.149639	0.075072	3.492%
"MV" is the evaluated solution mean value							"Std" is the evaluated solution standard deviation						
*Data y_0 and s_0 grouped in blocks of three. They were generated by Monte Carlo with model $y = \exp(cx)$ and $c = 1$, $x_0 = 1$, and Std Dev $x = 0.3$. Differences seen in y_0 and s_0 therefore correspond to stochastic differences arising from sampling x . Three different numbers of sampling histories $K = 500000, 100000$, and 10000 are used. Finally "Overlap" is calculated numerically for UMC-G+.													

Fig 16: Summary of GLS, UMC-G+, and UMC-B evaluations for test examples.

The blocks of three sets of results shown in this figure correspond to identical input data (y_0, s_0) and (y_e, s_e) but independent stochastic calculations using the indicated numbers of histories (note that $NHIST = K$). These repeated calculations with the same input data test stochastic stability for a given fixed input. There are several interesting observations to be made regarding Fig. 16. It is evident that the computed values $MV\{y\}$ and $Std\{y\}$, labelled simply as MV and Std in Fig. 16, agree very well with each other within each category of three independently computed results, regardless of the numbers of histories. Of course, even $NHIST = 10000$ would appear to constitute a rather large number of samples.

Comparisons between UMC-G+ and GLS results have already been discussed, so the present focus is on comparing UMC-G+ and UMC-B. In principle, at least for a very large number of histories, the corresponding values, i.e., for MV or Std, should be nearly the same. Therefore, the interest is in observing the differences that arise when NHIST is not so large. The mean values tend to agree reasonably well in all cases, at least within <3%. The largest differences occur in situations that involve the smallest magnitudes of factor “Overlap”, as might be expected based on considering Fig. 1. However, there are significant differences between UMC-G+ and UMC-B seen in Fig. 16 for the predicted standard deviations. In some cases they amount to as much as a factor of two.

The important point to remember here is that in UMC-B the stochastic sampling of potential solutions in space $S\{y\}$ is governed entirely by the prior probability function $p_0(y)$ while the likelihood factor, based on $L(y)$, serves only to weight these chosen possibilities for the final solution. On the other hand, the sampling processes in UMC-G or UMC-G+, which incorporate the posterior function $p(y)$, treat both the prior probability $p_0(y)$ and the likelihood function $L(y)$ on an equal footing in the sampling process. These observations, and the numerical results from the present investigation, suggest the following conclusions regarding application of the UMC-B approach to data evaluation:

To apply UMC-B successfully with a limited number of sampling histories there needs to be a robust value of factor “Overlap” signifying that the data being evaluated are reasonably consistent. If that is not the case, a very large number of sampling histories is likely to be needed to insure reliability of the final solution. Again, the occurrence of a small value for “Overlap” signals that the data being evaluated are inconsistent and the source of the discrepancy should therefore be investigated by the evaluator.

6. Summary

The present work demonstrates that considerable insight into stochastic and probability function shape effects that impact on applications of three distinct approaches to data evaluation using Unified Monte Carlo (UMC) can be acquired from simple numerical studies involving just a single variable to be evaluated and two input data values, one a “theoretical” model-calculated one and the second an “experimental” one. Noticeable differences in the evaluated results, depending on circumstances, have been observed between the predictions of the Monte Carlo methods UMC-G+ and UMC-B and GLS. In the simple examples considered here, where the data and variable to be evaluated are all comparable, UMC-G, which assumes normal prior and likelihood probability functions, yields identical results to GLS. A common thread in those cases where noticeable disagreements are seen between UMC-G+ and/or UMC-B and comparable GLS results is that the data being evaluated have large uncertainties and/or are basically inconsistent, as suggested by the given uncertainties. Thus, there is a premium on possessing good quality, consistent data, both theoretical and experimental, if one hopes to produce reliable evaluated results. This observation is certainly consistent with common sense.

References

- [1] D.L. Smith, Probability, Statistics, and Data Uncertainties in Nuclear Science and Technology, American Nuclear Society, LaGrange Park, IL (1991).
- [2] K.G. Gauss, Reprint: Theory of Motion of the Heavenly Bodies, Dover, NY (1963).
- [3] A. Legendre, Nouvelles Methodes pour la Determination des Orbites des Cometes, Paris (1805).
- [4] C.E. Shannon, Bell Syst. Tech. Journal **27** (1948) 379 and 623.
- [5] E.T. Jaynes, Where Do We Stand on Maximum Entropy, The Maximum Entropy Formalism (Eds. R.D. Legine and M. Tribus), M.I.T. University Press, Cambridge, MA (1978).
- [6] Rev. Thomas Bayes, An Essay Towards Solving a Problem in the Doctrine of Chance, published posthumously based on letters from the Rev. Bayes estate transmitted by Richard Price in a letter to John Canton, A. M. F. R. S. (1763). This document is available on the Internet at <http://www.stat.ucla.edu/history/essay.pdf>.
- [7] R.W. Peelle, Peelle's Pertinent Puzzle, Unpublished Memorandum, Oak Ridge National Laboratory (13 October 1987).
- [8] A.D. Carlson, *et al.*, International Evaluation of Neutron Cross Section Standards, Nucl. Data Sheets **110** (2009) 3215.
- [9] D.L. Smith, Covariance Matrices for Nuclear Cross Sections Derived from Nuclear Model Calculations, Report ANL/NDM-159, Argonne National Laboratory (2004).
- [10] A. Koning and D. Rochman, Ann. Nucl. Energy **35** (2008) 2024.
- [11] D.L. Smith, A Unified Monte Carlo Approach to Fast Neutron Cross Section Data Evaluation, Proceedings of the Eighth International Topical Meeting on Nuclear Applications and Utilization of Accelerators (AccApp'07), Pocatello, Idaho, July 29 – August 2, 2007, American Nuclear Society, LaGrange Park, IL (2007) 736.
- [12] R. Capote and D.L. Smith, An Investigation of the Performance of the Unified Monte Carlo Method of Neutron Cross Section Data Evaluation, Nucl. Data Sheets **109** (2008) 2768.
- [13] R. Capote and D.L. Smith, Unified Monte Carlo and Mixed Probability Functions, Proceedings of the International Conference on Nuclear Data for Science and Technology, April 26-30, 2010, Jeju, Korea. J. Korean Phys. Society **59** (2011) 1284.
- [14] R. Capote, D.L. Smith, and A. Trkov, Nuclear Data Evaluation Methodology Including Estimates of Covariances, EPJ Web of Conferences **8** (2010) 04001.
- [15] R. Capote *et al.*, Fourth International Symposium on Reactor Dosimetry (ISR-14), Bretton Woods, ASTM STP-1550, 179 (2012). See also: Journal of the ASTM International **9**(4), JAI 104119 (2012).
- [16] N. Metropolis, *et al.*, J. Chem. Phys. **21** (1953) 1087. See also: W.K. Hastings, Biometrika **57** (1970) 97.
- [17] D.L. Smith and J.W. Meadows, Nucl. Sci. Eng. **58** (1975) 314. These data are available from EXFOR: 10238.
- [18] D.L. Smith, *et al.*, Nucl. Instrum. Methods Phys. Res. **A488** (2002) 342.
- [19] MATLAB: The Language of Technical Computing, Mathworks Corporation: Internet https://www.mathworks.com/help/pdf_doc/matlab/matlab_prog.pdf.
- [20] Wikipedia: Internet https://en.wikipedia.org/wiki/Log-normal_distribution.
- [21] John D. Cook, Singular Value Consulting (29 October 2012). Internet: <http://www.johndcook.com/blog/2012/10/29/product-of-normal-pdfs/>.

Nuclear Data Section
International Atomic Energy Agency
Vienna International Centre, P.O. Box 100
A-1400 Vienna, Austria

E-mail: nds.contact-point@iaea.org
Fax: (43-1) 26007
Telephone: (43-1) 2600 21725
Web: <http://www-nds.iaea.org>
